Cardiac adenylyl cyclase overexpression precipitates and aggravates age-related myocardial dysfunction

Nathalie Mougenot, Delphine Mika, Gabor Czibik, Elisabeth Marcos, Shariq Abid, Amal Houssaini, Benjamin Vallin, Aziz Guellich, Hind Mehel, Daigo Sawaki, et al.

Cardiac adenylyl cyclase overexpression precipitates and aggravates age-related myocardial dysfunction

Nathalie Mougenot[1*], Delphine Mika[2*], Gabor Czibik [3,4], Elizabeth Marcos[3,4], Shariq Abid[3,4], Amal Houssaini[3,4], Benjamin Vallin[5], Aziz Guellich[2], Hind Mehel[2], Daigo Sawaki[2,3], Grégoire Vandecasteele[2], Rodolphe Fischmeister[2], Roger J. Hajjar[7], Jean-Luc Dubois-Randé[3,4], Isabelle Limon[5], Serge Adnot[3,4], Geneviève Derumeaux[3,4#] and Larissa Lipskaia[3,4,6#]

1. PECMV, INSERM, UMS28, Paris 6, Paris, France;
2. INSERM, UMR-S1180, Univ. Paris-Sud, Université Paris-Saclay, Châtenay-Malabry, France
3. INSERM, U955 and Département de Physiologie, Hôpital Henri Mondor, AP-HP, DHU ATVB, 94010, Créteil, France
4. Université Paris-Est, Faculté de Médecine, Créteil, France
5. Sorbonne Université Institute of Biology Paris-Seine, B2A, UMR8256, Paris, France
6. Cardiovascular Research Center, Icahn School of Medicine at Mount Sinai, New York, NY 10029, USA

* NM and DM contributed equally

GD and LL shared senior authorship

Short title: Cardiac adenylyl cyclase overexpression and aging

Corresponding author:
Larissa Lipskaia
INSERM, U955, Equipe 8,
Faculté de Médecine de Créteil
8 Rue du Général Sarrail,
94010, Créteil cedex, France
E-mail: larissa.lipskaia@inserm.fr

Tel.: +33 149 812 677; Fax: +33 149 812 667

Word count: 6560

TOC category – Prevention

TOC subcategory – Aging, Cardiovascular Disease

Abstract

Aims Increase of cardiac cAMP bioavailability and PKA activity through adenylyl-cyclase 8 (AC8) overexpression enhances contractile function in young transgenic mice (AC8TG). Ageing is associated with decline of cardiac contraction partly by the desensitization of β-adrenergic/cAMP signaling. Our objective was to evaluate cardiac cAMP signaling as age increases between 2 and 12 months and to explore whether increasing the bioavailability of cAMP by overexpression of AC8 could prevent cardiac dysfunction related to age.

Methods and Results Cardiac cAMP pathway and contractile function were evaluated in AC8TG and their non-transgenic littermates (NTG) at 2-mo and 12-mo-old. AC8TG demonstrated increased AC8, PDE1, 3B and 4D expression at both ages, resulting in increased PDE and PKA activity, and increased phosphorylation of several PKA targets including SERCA2a cofactor phospholamban (PLN) and GSK3α/β, a main regulator of hypertrophic growth and aging. Confocal immunofluorescence revealed that the major phospho-PKA substrates were co-localized with Z-line in 2 mo-old NTG but with Z-line interspace in AC8TG, confirming the increase of PKA activity in the compartment of PLN/SERCA2a. In both 12-mo-old NTG and AC8TG, PLN and GSK3α/β phosphorylation was increased together with main localization of phospho-PKA substrates in Z-line interspaces. Hemodynamics demonstrated an increased contractile function in 2-mo and 12-mo-old AC8TG, but not in NTG. By contrast echocardiography and Tissue Doppler Imaging (TDI) performed in conscious mice unmasked myocardial dysfunction with a decrease of systolic strain rate in both old AC8TG and NTG. In AC8TG TDI showed a reduced strain rate even in 2-mo-old animals. Development of age-related cardiac dysfunction was accelerated in AC8TG, leading to HF and premature death. Histological analysis confirmed early cardiomyocyte hypertrophy and interstitial fibrosis in AC8TG as compared with NTG.
Conclusions Our data demonstrated an early and accelerated cardiac remodeling in AC8TG mice, leading to the development of HF and reduced lifespan. Age-related reorganization of cAMP/PKA signaling can accelerate cardiac ageing, partly through GSK3α/β phosphorylation.

Keywords cAMP ● adenylyl cyclase 8 ● cardiac function ● aging ● transgenic mice

1. Introduction

A gradual decrease in left ventricle (LV) function and increase in LV mass are the hallmarks of an ageing heart[1, 2]. The decline of cardiac performance with ageing may result from a reduction in intrinsic contractile properties due to many factors. These factors include changes in excitation-contraction coupling due to desensitization of the β-adrenergic signaling pathway, with the downregulation of β_1-adrenergic receptors (β_1-ARs) and adenylyl-cyclases (ACs), slower calcium transport *via* the cardiac sarcoplasmic reticulum (SR) due to downregulation of the sarco(endo)plasmic-reticulum-calcium-ATPase (SERCA2a), impairment of mitochondrial function and alterations of contractile proteins expression[1-3]. The apparent deficit in sympathetic modulation of cardiac function with ageing occurs in the presence of elevated catecholamine levels due to age-related activation of sympathetic nervous system and reduced plasma clearance[4].

In cardiomyocytes, cAMP is an important regulator of contractile function[5]. Its production is activated by catecholamines binding to β_1-ARs, catalyzed by ACs, and its degradation is mediated by phosphodiesterases (PDEs)[5]. By activating PKA, cAMP induces the phosphorylation of key proteins such as L-type Ca^{2+} channels (LTCC), ryanodine-receptor-type 2 (RyR2), phospholamban (PLN), a negative regulator of SERCA2a, and troponin-I. This translates into strong positive inotropic, lusitropic and chronotropic responses. While it has been speculated several decades ago that activating the β-AR pathway might be beneficial in patients with heart failure (HF)[6], this hypothesis is no longer valid. Studies in transgenic (TG) mouse overexpressing either the β_1- or β_2-ARs, or the αs subunit of heterotrimeric G proteins (Gαs) in the heart display enhanced ventricular contractility at baseline and under β-AR stimulation, but develop a severe dilated cardiomyopathy with age, with a loss of myocytes and widespread interstitial fibrosis, resulting in lower survival rates[7]. Such age-related cardiac dysfunction might be related to β-AR activation of various effectors mediating hypertrophy, apoptosis and arrhythmia. These include the exchange protein directly activated by cAMP (EPAC)[8] and PKA substrates such as glycogen-synthase-kinase-3α/β (GSK3a/β)[9] and extracellular signal-regulated kinase 1/2 (ERK1/2)[10]. Since transgenic mice with cardiac overexpression of AC6 isoform do not exhibit such abnormalities[11-16], we hypothesized that targeting specific AC isoforms might perhaps be useful for preventing age-related cardiac dysfunction.

In the heart, the main AC isoforms responsible for catecholamine-dependent cAMP synthesis are AC5 and AC6. Our group has shown that increased AC5/6 expression during development is associated with a contractile phenotype[17], whereas the levels of these isoforms decrease during ageing and HF[5]. The AC6 isoform is localized in the plasma membrane outside the t-tubular region and is responsible for the β_1-AR stimulation of the LTCC current $I_{Ca,L}$, whereas the AC5 isoform is localized mainly in the t-tubular region and involved in β_2-AR signaling[18, 19]. Two additional isoforms, AC1 and AC8, were identified in sinoatrial node cells[20]. Unlike AC5/6 which are inhibited by Ca^{2+}, the AC8 isoform is stimulated by Ca^{2+} acting *via* calmodulin and is insensitive to Gαs *in vitro*[21]. AC8 expression in pacemaker cells allows PKA-dependent phosphorylation of Ca^{2+} cycling proteins that contributes to the generation of action potential[20]. Compartmentalization of signaling pathways driven by different Ca^{2+}-sensitive ACs isoforms is based on the evidence that ACs act as central foci of cAMP microdomains, binding directly or indirectly, *via* A kinase anchoring proteins (AKAPs), numerous regulatory and effector proteins such as PDEs, PKA, PKC and calcineurin (PP2B)[22, 23]. Of note, functional reorganization of receptor-associated cAMP microdomains leading to altered cAMP signal propagation was reported in hypertrophied and failing cardiomyocytes[24-26].

However, little is known about age-associated functional reorganization of cAMP/PKA/PDE signaling in cardiomyocytes. The question is of interest also because increased cAMP bioavailability could support contractile function in aged heart, despite the age-related desensitization of the β-AR signaling. Transgenic mice (AC8TG) with cardiac overexpression of Ca^{2+}/calmodulin–stimulated AC8 were created in order to increase the bioavailability of cardiac cAMP independent from β-AR stimulation[21]. Previously we have reported augmented PKA activity and enhanced cardiac function in young adult AC8TG mice, including increased LV systolic pressure, heart rate (HR), relaxation and sensitivity to external Ca^{2+}[21, 27, 28]. AC8-related cAMP appears to be confined at the level of longitudinal reticulum (LR), leading to large increase in SR Ca^{2+} transients and contraction, without an effect on LTCC current amplitude. This is due to the higher levels of activity of PDE1, 3 and 4 isoforms in AC8TG mice that shield LTCC from cAMP produced by AC8[27]. Given the beta adrenergic desensitization with age we hypothesized that increasing downstream cAMP levels through overexpression of AC8 would alleviate cardiac remodeling and dysfunction in the aged heart.

Here, we took advantage of the interesting model of AC8TG mice to investigate the impact of ageing on 1) the remodeling of the cAMP/PKA signaling pathway and 2) the effects of AC8 overexpression on cardiac function. As opposed to our expectations we found evidence for cardiac dysfunction occurring at an early stage of ageing which was associated with altered subcellular PKA distribution. This redistribution of PKA then is likely to be behind the hyperphosphorylation of PLN observed, in effect aiming to compensate for the loss of SERCA2a. Myocardial cAMP overproduction at the level of LR and subsequent PKA-dependent phosphorylation of GSK-3α/β are probably accountable for precipitating structural remodeling and cardiac dysfunction, ultimately leading to the development of HF and reduced lifespan.

2. Materials and Methods

2.1 Animals

The animal procedures used conformed to the guidelines from Directive 2010/63/EU of the European Parliament on the protection of animals used for scientific purposes. All animal experiments were approved (ref.14/04/15-8D) by the Institutional Animal Care and Use Committee of the French National Institute of Health and Medical Research (INSERM)–U955, Créteil, France. For biochemical studies, mice were euthanized by cervical dislocation, hearts were removed and snap-frozen immediately after euthanasia. We used heterozygous transgenic mice with cardiac AC8 overexpression (AC8TG), obtained as previously described[21], and their control non-transgenic C57/Bl6 WT littermates (NTG) at two ages: 2- and 12-mo old.

2.2. Echocardiography

Closed-chest transthoracic echocardiography was performed in awaken mice with a 13-MHz linear-array transducer with a digital ultrasound system (Vivid 7, GE Medical Systems), as previously described[29]. Wall thickness and LV dimensions were obtained in M-mode, at the level of the papillary muscles; the LV mass, FS, and relative wall thickness were calculated. Strain rate curves were obtained from a parasternal short-axis view at mid-ventricular level, at a frame rate of 450 frames per second and a depth of 1 cm. Peak systolic radial strain rate (StR, s^{-1}) was computed from a region of interest positioned in the mid-posterior wall and was measured over an axial distance of 0.6 mm. Three consecutive cardiac cycles were selected and peak systolic velocities and peak StR were measured and

averaged. StR imaging analysis was performed offline (EchoPac Software, GE Medical Systems) by an observer blind to the age of the animals.

2.3 Invasive hemodynamics

After tracheal intubation, anesthetized mice (50mg/kg of sodium pentobarbital by i.p.) maintained at 37°C were connected to a rodent ventilator (Minivent Mouse ventilator type 845, Harvard Apparatus, frequency of 170 stokes/min and a volume of 200 µl for 30 g). Invasive hemodynamic measurements were performed with a pressure transducer catheter (size 1.4 F, Millar Micro-tip catheter transducer, model SPR-671; Millar Instruments, Inc, Houston, TX, USA), introduced into the right carotid artery and pushed into the LV. Pressures were recorded on a Gould recorder (Model RS 3200; Gould Instrument Systems, Ohio, USA). Measurements obtained were: systolic, diastolic and mean arterial blood pressure; LV pressure with positive and negative derivatives of pressure (LV dP/dt maximum and minimum), HR. Hemodynamic measurements were recorded at baseline and five minutes after the injection of incremental doses of isoproterenol (ISO, 1 to 100 µg/kg). At least ten sequential beats were averaged for each parameter. Then, the thorax was opened and the lungs and heart were removed and used for morphometric and histological analysis.

2.4 Morphometric and histological analysis

Hearts were removed (atria were separated from ventricles) and weighed for the calculation of heart-to-body weight ratio and heart weight-to-tibia length ratio. Ventricles were frozen in an embedding compound for cryosectioning (Tissue-Tek O.C.T) and used for histological analysis as described in supplemental methods.

2.5 Confocal Immunofluorescence Microscopy

Immunostaining was performed on frozen sections using primary antibodies anti-phospho-(Ser/Thr) PKA Substrate Antibody (#9621, Cell Signaling) and anti-alpha-Actinin (ab9465, Abcam) and secondary antibodies conjugated to Alexa-546 or Alexa-488 as described in supplemental methods.

2.6 cAMP and PKA kinase activity assay

[cAMP] was determined in cardiac tissues using the Mouse/Rat cAMP Parameter Assay Kit (Catalog No.KGE012B, R&D Systems). PKA (cAMP-dependent protein kinase) kinase activity was determined in cardiac tissues with the PKA Kinase Activity Assay Kit (Catalog No. ab139435, Abcam) according to manufacture instructions. 50 µg of total cardiac protein per well was used for assay.

2.7 PDE activity assay

PDE activity was measured according to the method of Thompson *et al.*[30], on myocardial protein extracts from 2 mo-old and 12 mo-old NTG and AC8TG mice (*n*=6 in each group). In brief, samples (20 µg of myocardial proteins) were assayed in a 200 µL reaction mixture containing 40 mM Tris-HCl (pH 8.0), 1 mM $MgCl_2$, 1.4 mM β-mercaptoethanol, 1 µM cAMP, 0.75 mg/mL bovine serum albumin, and 0.1 µCi of [^{3}H]cAMP (Perkin Elmer) for 25 minutes at 33°C in the presence or in the absence of IBMX (1mM) (Sigma Aldrich). The reaction was terminated by heat inactivation. The PDE reaction product 5'-AMP was then hydrolyzed by incubating the assay mixture with 50 µg of *Crotalus atrox* snake venom (Sigma Aldrich) for 20 minutes at 33°C, and the resulting nucleotide was then separated by anion exchange chromatography and quantified by scintillation counting. Total PDE activity was defined as a

fraction of [^{3}H]cAMP hydrolyzed and calculated as follow: ((sample count – blanc)/(total count – blanc)). IBMX-sensitive PDE activity was defined as the fraction of cAMP-PDE activity inhibited by 1 mM IBMX.

2.8 Protein and RNA analysis.

Protein and RNA extraction, immunoblotting and Real-time qPCR analysis were performed using standard techniques as described in supplemental methods.

2.9 Statistical analysis

Quantitative data are presented as individual values + mean or mean ± SEM, as indicated. Statistical significance was determined using two-way ANOVA for two variables, one-way ANOVA for multiple comparisons, or Student unpaired *t*-tests for comparisons between two groups. When ANOVA indicated significance, the groups were compared using a Newman-Keuls post-hoc test (Prism 6.0, GraphPad Software, San Diego, CA). A P value < 0.05 was considered statistically significant.

3. Results

3.1 Age-related alterations of cAMP/PKA pathway

To investigate the impact of AC8 on cAMP signaling with ageing, NTG and AC8TG mice were explored at the age of 2 and 12 months. First, we showed AC8 overexpression in both 2- and 12-mo-old AC8TG, whereas AC5 and AC6 were unchanged (**Figure 1A, B & C**). As expected, AC8 overexpression was associated with higher cardiac cAMP levels in both 2- and 12-mo-old AC8TG as compared with young NTG. Of note, ageing increased cAMP levels in both 12-mo-old AC8TG and NTG hearts as compared with young NTG (**Figure 1D**). Since PDEs control local cAMP levels, we analyzed the expression of the main cardiac isoforms. We found an increased expression of PDE1A&C, PDE3B and PDE4D isoforms in 2- and 12-mo-old AC8TG (**Figure 1E, F, I & L**) in line with previously reported increase of PDE1, 3 and 4 activities in young AC8TG[27] . We also observed higher total and IBMX-sensitive PDE activity in 2- and 12-mo-old AC8TG (**Figure 2A&B**). While PDE isoform transcript levels were not modified in 12-mo-old NTG (**Figure 1E-L**), the total and IBMX-sensitive PDE activities were increased (**Figure 2A&B**). Consistent with our previous observations[21], we demonstrated an increase in cardiac PKA activity in 2- and 12-mo-old AC8TG mice, but not in 12-mo old NTG (**Figure 2C**).

Increase in cardiac cAMP levels and PDE activity in 12-mo-old NTG might suggest altered cAMP confinement compensating for age-related cardiac dysfunction[25, 26]. Therefore we assessed if PKA substrates were differently phosphorylated and found increased phosphorylation of several, but not all, PKA substrates in 12-mo-old NTG and AC8TG, in addition to 2-mo-old AC8TG hearts (**Figure 2D & E**). Furthermore these changes were associated with a different localization of PKA substrates between young NTG and the other groups. Indeed, AC8TG mice exhibited an "ageing" distribution of phospho-PKA substrates, similar to old NTG and mainly in Z-line interspaces, confirming the increase of PKA activity in the compartment of PLN/SERCA2a (LR). In young NTG, phospho-PKA substrates were co-localized with Z-line, suggesting RyR2 and LTCC to be the principal PKA targets in young cardiomyocytes (**Figure 2F**).

In line with the distribution of phospho-PKA substrates, (S16)-phosphorylation of PLN similarly increased in both 2- and 12-mo-old AC8TG mice and in 12-mo-old NTG (**Figure 3A** & **B**). As SERCA2a activity is critically regulated by cAMP-responsive PLN and its downregulation is recognized as a major feature of both aged heart and HF, we further examined SERCA2a expression. We confirmed the downregulation of SERCA2a in 12-mo-old NTG mice. Intriguingly, we also found a downregulation of SERCA2a as early as 2-mo-old in AC8TG compared to young NTG animals and reaching similar levels as in 12-mo-old AC8TG (**Figure 3A** & **B**).

We finally immunoblotted for GSK3α/β, ERK1/2 or the cAMP response element binding protein (CREB) which are PKA targets and regulators of cell growth and metabolism[10]. Western blot analysis revealed an increased GSK3α/β phosphorylation in both 2- and 12-mo-old AC8TG and in 12-mo-old NTG whilst total GSK3α/β expression remained unchanged (**Figure 3C&D**). The lack of difference in Thr308 or Ser473 Akt1 phosphorylation along with both expression and phosphorylation of CREB1 and ERK1/2 (not shown) made us speculate on a specific involvement of PKA-dependent GSK3α/β activation in the gross phenotype (**Figure 3E&F**).

3.2 Contractile function in ageing animals

Further to our previous data on enhanced cardiac function in young AC8TG mice[21, 28], we compared *in vivo* hemodynamic function in 2-mo- and 12-mo-old NTG and AC8TG mice (**Figure 4, Supplemental Table 1)**. Under basal conditions we found that *i)* heart rate (HR) was higher in AC8TG than in NTG mice in both age groups **(Figure 4A)**; *ii)* LV contractility (LV dP/dt_{max}) were twice as high in 2-mo-old AC8TG as in 2-mo-old NTG mice (**Figure 4B & C**); and *iii)* there was still a 30% increase in dP/dt_{max} in 12-mo-old AC8TG compared to 12-mo-old NTG mice (**Figure 4C**). In NTG mice, β-AR stimulation with isoprenaline (ISO) induced the expected dose-dependent stimulation of HR and LV contractility, even in 12-mo-old NTG animals (**Figure 4A, C & D**). By contrast, β-AR stimulation did not increase HR in AC8TG mice of either age, but markedly decreased dP/dt_{max} in young AC8TG and did not change it in 12-mo-old AC8TG mice (**Figure 4A, C & D**).

Next, we have investigated evolution of cardiac morphology and function with age in NTG and AC8TG mice, by performing cross-sectional echocardiography in conscious mice from three age groups (2 mo-old, 6 mo-old and 12 mo-old) (**Figure 5**). HR was higher in young AC8TG than in young NTG animals and did not change with age in AC8TG mice, but increased with age in NTG mice (**Figure 5A**). As expected, ageing was accompanied by alteration of cardiac function with a progressive increase in LV dimensions (**Figure 5B**) and a deterioration of LVEF in both NTG and AC8TG (**Figure 5C**). Strain rate (StR), a sensitive index of regional myocardial contractility, identified reduced regional contractile function as early as 2 mo-old in AC8TG mice, and confirmed the progressive decline of systolic function with age in both NTG and AC8TG group (**Figure 5D**). Those results obtained in cross-sectional study were confirmed in a longitudinal follow-up study performed in mice between the age of 2 and 14 months (**Supplementary Figure 1)**.

Furthermore lifespan monitoring revealed an increased mortality rate of AC8TG mice with median life span of 17 months as compared with over 24 months for NTG mice (75% still alive at 24 months) (**Supplementary Figure 2**).

3.3 Impact of ageing on myocardial structure

Both morphometric analysis and qRT-PCR analysis confirmed age-related cardiac remodeling with increase of HW and HW/TL ratio in AC8TG mice (**Table 1, Figure 6A**) and increase of β-myosin heavy chain expression (**Figure 6B**), respectively. However, the expression of the atrial natriuretic peptide (ANP) increased only in aged AC8TG mice suggesting a HF phenotype (**Figure 6C**). Furthermore, liver (1471 ± 175 *vs.* 1924 ± 98 mg, $P<0.05$) and lung (204 ± 11 *vs.* 257 ± 13 mg, $P<0.05$) weights were higher in the 12-mo-old AC8TG mice (n=10) than in the 12-mo-old NTG mice (n=10), indicating cardiac dysfunction.

In young AC8TG histological analysis identified early alterations of myocardial structure, with cardiomyocyte hypertrophy and endocardial fibrosis (**Figure 6D & E**). This increased with ageing while interstitial fibrosis extended towards epicardium (**Figure 6D & E**). Conversely, such abnormalities were observed only in 12-mo-old NTG, but not in young mice (**Figure 6D & E**).

4. Discussion

In this study we demonstrated that age-dependent cardiac remodeling is accelerated and exaggerated in AC8TG leading to myocardial dysfunction, development of HF and premature death.

Our data confirm the impact of ageing on the heart and the major role of the fibrotic process associated with myocyte loss and hypertrophy of the remaining myocytes leading to contractile dysfunction[1, 2, 31]. Indeed in NTG animals, echocardiography combined with TDI revealed a progressive increase in LV dimension together with a decrease in LVEF and systolic strain rate with ageing, consistent with our previous observations[29]. These changes in systolic function were associated with an increase in myocardial collagen content in endocardial but not epicardial layers.

Our results confirm age-related impact on cardiac function and remodeling such as cardiomyocyte hypertrophy associated with an increased GSK3 phosphorylation and decrease in SERCA2a expression in hearts[32, 33]. They also unmask an unexpected channeling of cAMP/PKA towards PLN/SERCA2a compartment, as demonstrated by the increase in the phosphorylation of PKA substrates and PDE activities similar to that observed in AC8TG mice. The novelty of our data consists in the demonstration that modification of PDE/cAMP signaling in aged heart, presumably aiming to compensate the loss of SERCA2a, is hampered by PKA-dependent phosphorylation of GSK3α/β that may be responsible, along with other actors, for age-related cardiac remodeling. Indeed, the GSK3β is known to be the main regulator of cardiac hypertrophic remodeling via calcineurin/NFAT signaling pathway, whereas GSK3α promotes cardiac ageing *via* activation of mTOR[9]. Other relevant factors, particularly those directly activated by cAMP factor EPAC, calcium activated CaMKII or PKA downstream phosphatase PP1 and inhibitor of protein phosphatase-I (I-1), may also be involved in myocardial ageing.

Since the age-related cardiac dysfunction in NTG mice is characterized by a re-organization of the cAMP/PKA signaling pathway upstream of PLN, we hypothesized (**Figure 7**) that this reorganization can be achieved by channeling cAMP towards LR, similar to that described in the early compensated phase of heart disease[25, 26]. Thus, our results suggest that natural cardiac ageing is accompanied by a functional redistribution of cAMP compartments (i.e. available cAMP can be canalized towards PLN-containing microdomains) together with a shift of local (β_2-AR) towards global (β_1-AR) cAMP pool, β-AR desensitization and down-regulation of SERCA2a expression. The mechanism underlying this increase remains to be identified, but it may involve structural reorganization of the cardiomyocyte surface, including loss of T-tubules and the redistribution of β_1- and β_2-ARs, as previously reported in failing cardiomyocytes[24]. This mechanism probably compensates for the loss of SERCA2a and as such acutely adaptive, but becomes maladaptive on the long term.

The compartmentalization of cAMP signaling in cardiomyocytes depends on the anchoring of PKA to specific subcellular sites and the ability of PDEs to canalize cAMP towards these sites. The main four cardiac PDEs families responsible for cAMP hydrolysis (PDE1-4) are encoded by several genes and exhibit different subcellular localization[5, 34, 35]. The Ca^{2+}/calmodulin activated isoform, PDE1 is predominantly cytosolic[35], whereas PDE4B isoform is associated with LTCC complex and regulates $I_{Ca,L}$ during β-AR stimulation[34]. PDE4D is part of the RyR2 channel complex and also together with PDE3A1 is associated with PLN-SERCA2a complex and regulates Ca^{2+} reuptake in the SR[34, 35]. PDE3 and PDE4 activity is regulated by PKA phosphorylation thereby providing negative feedback to β-AR stimulation[36, 37]. The PDE3B interaction with PI3Kγ is thought to be important for the regulation of cardiac contractility and was found to affect cardiac hypertrophy in a mouse model of chronic pressure overload[38]. Under pathological conditions, numerous studies have reported alterations of expression and/or subcellular redistribution of cardiac PDE isoforms[34]. However to our knowledge, there has been no study investigating potential modifications of cardiac PDEs in the course of ageing. The modification of PDE activity observed here in aged NTG may be achieved through differential protein expression, phosphorylation by distinct kinases or posttranslational modifications[35].

We have reported previously that in young AC8TG cAMP produced by AC8 is specifically employed to increase SR Ca^{2+} transient amplitude and relaxation kinetics at the sarcolemma and has no effect on $I_{Ca,L}$[27]. Our present finding imply that this is achieved in part by increased PLN phosphorylation. We have also reported the specific increase of PDE1 (+124%), PDE3 (+27%) and PDE4 (+28%) in young AC8TG [27, 28]. In the present paper we have confirmed the increase of total PDE activity supported by the up-regulation of the predominantly cytosolic PDE1A&1C and the membrane associated PDE3B and PDE4D isoforms in AC8TG regardless of age. Our results suggest that in AC8TG cardiomyocytes AC8 is located within lipid-rich microdomains proximal to longitudinal SR/PM junctions delimited by PDE1, PDE3B and PDE4D and containing the SERCA2a and its cofactor PLN (**Figure 7**). Further studies, employing subcellular cAMP measurements in cardiomyocytes should be performed to decipher the function of such compartments containing this Ca^{2+}-operated AC isoform.

In AC8TG mice SERCA2a is downregulated well before the development of any signs of HF. It can therefore be considered as a mechanism of adaptation to the continuous increase in SERCA2a activity triggered by the phosphorylation of PLN. In this context modifications of cAMP signaling in young AC8TG mice can be compared with those occurring during compensated stage of cardiac disease, becoming decompensated with ageing. This process is very similar to the first phase of HF compensation in the presence of high levels of circulating catecholamines, in which signs of HF are not detectable by conventional echocardiography due to physiological and molecular adaptations. However excessive β-AR stimulation and cAMP production can also activate pathological hypertrophic remodeling in part *via* PKA-dependent GSK3α/β phosphorylation. Moreover, EPAC can also be in part responsible for drastic age-related cardiac remodeling in AC8TG.

We also found that cardiac remodeling and premature ageing in young AC8TG animals, leading to reduced median lifespan. Whereas traditional measures of echocardiography found no signs of impaired cardiac function in young AC8TG animals, tissue Doppler imaging revealed reduced myocardial strain rate compared to young NTG mice. These data indicate that the regional contractility assessed by strain rate was compromised even in young AC8TG. With regard to the development of HF in AC8TG mice with reduced lifespan, these early molecular and functional abnormalities may predict HF.
Our data provide an important piece of evidence against the strategy consisting in targeting and enhancing β-AR downstream effectors for preventing HF and age-related cardiac dysfunction. Indeed, we demonstrate the worsening of cardiac function resulting in progressive cardiomyopathy and

premature death in aged mice with cardiac overexpression of AC8 isoform. We previously reported the strong compartmentation of the AC8-dependent increase in cAMP levels in cardiomyocytes that translated into functional effects only in conditions of β-AR stimulation[21, 27, 28]. Since AC8 overexpression in cardiomyocytes specifically accelerates Ca^{2+} re-uptake in the SR, by increasing SERCA2a activity through PKA-mediated phosphorylation of the PLN without affecting Ca^{2+} influx into the cell[27], one might consider that increasing Ca^{2+} uptake from the SR without increasing Ca^{2+} influx at the SR is beneficial to contractile function[27]. However, numerous TG models with chronic activation of the cAMP pathway in the heart (overexpressing β_1-AR, β_2-AR, Gαs, PKA, I-I, etc) display enhanced cardiac function in young animals but evolving towards progressive cardiomyopathy and premature death with age (reviewed in[7]).

In conclusion, using a cardiac overexpression of AC8 isoform we demonstrated that the increase of cardiac cAMP bioavailability and PKA activity precipitates and aggravates age-related myocardial dysfunction. Using systolic strain rate for assessing myocardial function we revealed early myocardial dysfunction in young AC8TG mice. Finally, we have demonstrated modifications of cAMP/PKA signaling in normal aged cardiomyocytes resulting in increased phosphorylation of PLN and GSK3α/β by PKA. Whereas PLN phosphorylation is possibly a beneficial adaptation aiming to compensate for the loss of SERCA2a in ageing cardiomyocytes and rescue defective contractile function, it becomes maladaptive in the long term. The excessive PKA activation is hampered by induction of the hypertrophy-, fibrosis- and age-related GSK3α/β signaling pathways and may play a role in pathological hypertrophic remodeling and accelerated ageing.

Funding

This work was supported by INSERM, *Délégation à la Recherche Clinique de l'AP-HP*, *Agence Nationale de la Recherche* (ANR Grant 11 BSV1 034 01), AREM CAR foundation, NIH R01HL117505, HL119046, HL129814, 128072, a P50 HL112324 and a Leducq Transatlantic Foundation grant. INSERM U1180 is a member of the Laboratory of Excellence LERMIT supported by a grant from ANR (ANR-10-LABX-33) under the program "Investissements d'Avenir" ANR-11-IDEX-0003-01. DM was supported by a JC/JC starting grant from ANR (ANR-16-CE14-0014).

Acknowledgments

We thank the Gene Therapy Resource Program (GTRP) of the National Heart, Lung, and Blood Institute, National Institutes of Health, USA. We also thank Dr S. Morosan (UMS28 Director) and C. Enond (Animal Facility Manager, NAC, UMS28, Paris-6, Paris, France). We thank Dr Natalie Fournier (EA4529, Univ. Paris-Sud, Université Paris-Saclay) for her help with radioactivity management.

Disclosures

None

References

1. Lakatta EG, Levy D. Arterial and cardiac aging: major shareholders in cardiovascular disease enterprises: Part I: aging arteries: a "set up" for vascular disease. *Circulation* 2003;**107**:139-146.
2. Lakatta EG, Levy D. Arterial and cardiac aging: major shareholders in cardiovascular disease enterprises: Part II: the aging heart in health: links to heart disease. *Circulation* 2003;**107**:346-354.
3. Lipskaia L, Chemaly ER, Hadri L, Lompre AM, Hajjar RJ. Sarcoplasmic reticulum Ca(2+) ATPase as a therapeutic target for heart failure. *Expert Opin Biol Ther* 2010;**10**:29-41.
4. Fleg JL, Strait J. Age-associated changes in cardiovascular structure and function: a fertile milieu for future disease. *Heart Fail Rev* 2012;**17**:545-554.
5. Guellich A, Mehel H, Fischmeister R. Cyclic AMP synthesis and hydrolysis in the normal and failing heart. *Pflugers Arch* 2014;**466**:1163-1175.
6. Dorn GW, 2nd, Molkentin JD. Manipulating cardiac contractility in heart failure: data from mice and men. *Circulation* 2004;**109**:150-158.
7. El-Armouche A, Eschenhagen T. Beta-adrenergic stimulation and myocardial function in the failing heart. *Heart Fail Rev* 2009;**14**:225-241.
8. Morel E, Marcantoni A, Gastineau M, Birkedal R, Rochais F, Garnier A, Lompre AM, Vandecasteele G, Lezoualc'h F. cAMP-binding protein Epac induces cardiomyocyte hypertrophy. *Circ Res* 2005;**97**:1296-1304.
9. Lal H, Ahmad F, Woodgett J, Force T. The GSK-3 family as therapeutic target for myocardial diseases. *Circ Res* 2015;**116**:138-149.
10. Chruscinski AJ, Singh H, Chan SM, Utz PJ. Broad-scale phosphoprotein profiling of beta adrenergic receptor (beta-AR) signaling reveals novel phosphorylation and dephosphorylation events. *PLoS One* 2013;**8**:e82164.
11. Lai NC, Roth DM, Gao MH, Tang T, Dalton N, Lai YY, Spellman M, Clopton P, Hammond HK. Intracoronary adenovirus encoding adenylyl cyclase VI increases left ventricular function in heart failure. *Circulation* 2004;**110**:330-336.
12. Roth DM, Bayat H, Drumm JD, Gao MH, Swaney JS, Ander A, Hammond HK. Adenylyl cyclase increases survival in cardiomyopathy. *Circulation* 2002;**105**:1989-1994.
13. Roth DM, Gao MH, Lai NC, Drumm J, Dalton N, Zhou JY, Zhu J, Entrikin D, Hammond HK. Cardiac-directed adenylyl cyclase expression improves heart function in murine cardiomyopathy. *Circulation* 1999;**99**:3099-3102.
14. Tang T, Gao MH, Roth DM, Guo T, Hammond HK. Adenylyl cyclase type VI corrects cardiac sarcoplasmic reticulum calcium uptake defects in cardiomyopathy. *Am J Physiol Heart Circ Physiol* 2004;**287**:H1906-1912.
15. Tang T, Hammond HK, Firth A, Yang Y, Gao MH, Yuan JX, Lai NC. Adenylyl cyclase 6 improves calcium uptake and left ventricular function in aged hearts. *J Am Coll Cardiol* 2011;**57**:1846-1855.
16. Lai NC, Tang T, Gao MH, Saito M, Takahashi T, Roth DM, Hammond HK. Activation of cardiac adenylyl cyclase expression increases function of the failing ischemic heart in mice. *J Am Coll Cardiol* 2008;**51**:1490-1497.
17. Lipskaia L, Grepin C, Defer N, Hanoune J. Adenylyl cyclase activity and gene expression during mesodermal differentiation of the P19 embryonal carcinoma cells. *J Cell Physiol* 1998;**176**:50-56.
18. Timofeyev V, Myers RE, Kim HJ, Woltz RL, Sirish P, Heiserman JP, Li N, Singapuri A, Tang T, Yarov-Yarovoy V, Yamoah EN, Hammond HK, Chiamvimonvat N. Adenylyl cyclase subtype-

specific compartmentalization: differential regulation of L-type Ca2+ current in ventricular myocytes. *Circ Res* 2013;**112**:1567-1576.
19. Wright PT, Nikolaev VO, O'Hara T, Diakonov I, Bhargava A, Tokar S, Schobesberger S, Shevchuk AI, Sikkel MB, Wilkinson R, Trayanova NA, Lyon AR, Harding SE, Gorelik J. Caveolin-3 regulates compartmentation of cardiomyocyte beta2-adrenergic receptor-mediated cAMP signaling. *J Mol Cell Cardiol* 2014;**67**:38-48.
20. Vinogradova TM, Lakatta EG. Regulation of basal and reserve cardiac pacemaker function by interactions of cAMP-mediated PKA-dependent Ca2+ cycling with surface membrane channels. *J Mol Cell Cardiol* 2009;**47**:456-474.
21. Lipskaia L, Defer N, Esposito G, Hajar I, Garel MC, Rockman HA, Hanoune J. Enhanced cardiac function in transgenic mice expressing a Ca(2+)-stimulated adenylyl cyclase. *Circ Res* 2000;**86**:795-801.
22. Cooper DM. Store-operated Ca(2)(+)-entry and adenylyl cyclase. *Cell Calcium* 2015;**58**:368-375.
23. Halls ML, Cooper DM. Adenylyl cyclase signalling complexes - Pharmacological challenges and opportunities. *Pharmacol Ther* 2017;**172**:171-180.
24. Nikolaev VO, Moshkov A, Lyon AR, Miragoli M, Novak P, Paur H, Lohse MJ, Korchev YE, Harding SE, Gorelik J. Beta2-adrenergic receptor redistribution in heart failure changes cAMP compartmentation. *Science* 2010;**327**:1653-1657.
25. Perera RK, Sprenger JU, Steinbrecher JH, Hubscher D, Lehnart SE, Abesser M, Schuh K, El-Armouche A, Nikolaev VO. Microdomain switch of cGMP-regulated phosphodiesterases leads to ANP-induced augmentation of beta-adrenoceptor-stimulated contractility in early cardiac hypertrophy. *Circ Res* 2015;**116**:1304-1311.
26. Sprenger JU, Perera RK, Steinbrecher JH, Lehnart SE, Maier LS, Hasenfuss G, Nikolaev VO. In vivo model with targeted cAMP biosensor reveals changes in receptor-microdomain communication in cardiac disease. *Nat Commun* 2015;**6**:6965.
27. Georget M, Mateo P, Vandecasteele G, Jurevicius J, Lipskaia L, Defer N, Hanoune J, Hoerter J, Fischmeister R. Augmentation of cardiac contractility with no change in L-type Ca2+ current in transgenic mice with a cardiac-directed expression of the human adenylyl cyclase type 8 (AC8). *FASEB J* 2002;**16**:1636-1638.
28. Georget M, Mateo P, Vandecasteele G, Lipskaia L, Defer N, Hanoune J, Hoerter J, Lugnier C, Fischmeister R. Cyclic AMP compartmentation due to increased cAMP-phosphodiesterase activity in transgenic mice with a cardiac-directed expression of the human adenylyl cyclase type 8 (AC8). *FASEB J* 2003;**17**:1380-1391.
29. Derumeaux G, Ichinose F, Raher MJ, Morgan JG, Coman T, Lee C, Cuesta JM, Thibault H, Bloch KD, Picard MH, Scherrer-Crosbie M. Myocardial alterations in senescent mice and effect of exercise training: a strain rate imaging study. *Circ Cardiovasc Imaging* 2008;**1**:227-234.
30. Thompson WJ, Brooker G, Appleman MM. Assay of cyclic nucleotide phosphodiesterases with radioactive substrates. *Methods Enzymol* 1974;**38**:205-212.
31. Lakatta EG. Arterial and cardiac aging: major shareholders in cardiovascular disease enterprises: Part III: cellular and molecular clues to heart and arterial aging. *Circulation* 2003;**107**:490-497.
32. Cain BS, Meldrum DR, Joo KS, Wang JF, Meng X, Cleveland JC, Jr., Banerjee A, Harken AH. Human SERCA2a levels correlate inversely with age in senescent human myocardium. *J Am Coll Cardiol* 1998;**32**:458-467.
33. Jiao Q, Takeshima H, Ishikawa Y, Minamisawa S. Sarcalumenin plays a critical role in age-related cardiac dysfunction due to decreases in SERCA2a expression and activity. *Cell Calcium* 2012;**51**:31-39.
34. Bobin P, Belacel-Ouari M, Bedioune I, Zhang L, Leroy J, Leblais V, Fischmeister R, Vandecasteele G. Cyclic nucleotide phosphodiesterases in heart and vessels: A therapeutic perspective. *Arch Cardiovasc Dis* 2016;**109**:431-443.

35. Bender AT, Beavo JA. Cyclic nucleotide phosphodiesterases: molecular regulation to clinical use. *Pharmacol Rev* 2006;**58**:488-520.
36. Shakur Y, Holst LS, Landstrom TR, Movsesian M, Degerman E, Manganiello V. Regulation and function of the cyclic nucleotide phosphodiesterase (PDE3) gene family. *Prog Nucleic Acid Res Mol Biol* 2001;**66**:241-277.
37. Leroy J, Abi-Gerges A, Nikolaev VO, Richter W, Lechene P, Mazet JL, Conti M, Fischmeister R, Vandecasteele G. Spatiotemporal dynamics of beta-adrenergic cAMP signals and L-type Ca2+ channel regulation in adult rat ventricular myocytes: role of phosphodiesterases. *Circ Res* 2008;**102**:1091-1100.
38. Patrucco E, Notte A, Barberis L, Selvetella G, Maffei A, Brancaccio M, Marengo S, Russo G, Azzolino O, Rybalkin SD, Silengo L, Altruda F, Wetzker R, Wymann MP, Lembo G, Hirsch E. PI3Kgamma modulates the cardiac response to chronic pressure overload by distinct kinase-dependent and -independent effects. *Cell* 2004;**118**:375-387.

Figure legends

Figure 1. Increased cardiac cAMP by AC8 overexpression induces a subset of counter-regulators PDEs. A-L. Scatter-plots showing either myocardial cAMP level (**D**) or the relative mRNA expression normalized to 18S mRNA of AC8 (**A**), AC5 (**B**), AC6 (**C**), PDE1A (**E**), PDE1C (**F**), PDE2A (**G**), PDE3A (**H**), PDE3B (**I**), PDE4A (**J**), PDE4B (**K**) or PDE4D (**L**) in NTG (○) and AC8TG (●) mice. The horizontal line indicates the mean value for each group. 8-10 animals were analyzed in each group. **P* <0.05; ***P* <0.01; ****P*<0.001 (one-way ANOVA followed by Newman-Keuls post-hoc test).

Figure 2. Altered localization of phospho-PKA substrates in the cardiomyocytes of AC8TG and ageing NTG animals. A, B, C. Scatter-plot showing the total (**A**) and IBMX-sensitive (**B**) cardiac PDE activity and basal cardiac PKA activity (**C**) in 2- and 12-mo-old NTG (○) and AC8TG (●) mice. **D, E**. Typical immunoblot (**D**) for the visualization of numerous of PKA substrates differently phosphorylated within 2-mo-old NTG and 12-mo-old NTG or AC8TG animals. Expression of three phosphorylated PKA-substrates (1, 2 and 3) was quantified in different groups of mice and normalized to GAPDH (**E**). The horizontal line indicates the mean value for each group. 8-10 animals were analyzed in each group. **P* <0.05; ***P* <0.01; ****P*<0.001 (one-way ANOVA followed by Newman-Keuls post-hoc test). **F.** Confocal immunofluorescence of phospho-PKA substrate on snap-frozen cardiac cross sections. Scale bars: 10 µm. Position of Z-lines, corresponding to T-tubule/junctional reticulum space, are indicated by alpha-actinin (α-Act) labelling (green). Z-line interspace corresponded to longitudinal reticulum containing SERCA2a/PLN. Preferential localizations of phosphorylated PKA substrates are indicated by labelling with anti-phospho-PKA substrate antibody (red). Line indicates the position of orthogonal views for each section. Three animals from each group were analyzed.

Figure 3. Altered phosphorylation of several PKA targets in AC8TG and ageing NTG animals includes p(S16) PLN, p(S21)-GSK-3α and p(S9)-GSK-3β. A, B. Typical immunoblot (**A**) and quantification (**B**) for the expression of p(S16)PLN, total PLN and SERCA2a in the heart. **C, D.** Typical immunoblot (**C**) and quantification (**D**) for the expression of Phospho-GSK3α/β (upper panel) and total GSK3α/β (down panel). Expression of GSK3 was normalized to GAPDH expression. **E, F.** Typical immunoblot (**E**) and quantification (**F**) for the expression of Phospho-Akt1(Ser473) and Phospho-Akt1(Thr308) in the heart. The horizontal line indicates the mean value for each group. 8-10 animals were analyzed in each group. **P* <0.05; ***P* <0.01; ****P*<0.001 (one-way ANOVA followed by Newman-Keuls post-hoc test).

Figure 4. Enhanced LV hemodynamics in young AC8TG evaluate towards normalized LV systolic pressure in aged AC8TG but blunted β-AR responsibility in both ages NTG and AC8TG mice. Hemodynamic recording was performed in 2-mo-old (n=9) and 12-mo-old (n=12) NTG and 2-mo-old (n=9) and 12-mo-old (n=15) AC8TG mice. The following parameters were measured in NTG (○) and AC8TG (●) mice at baseline and after isoproterenol (ISO) stimulation: HR (beats/min) (**A**); LVSP–LV systolic pressure (**B**); ΔP–LV pressure variation; dp/dt_{max} (**C**) and dp/dt_{min} (**D**). **E**. Typical traces of hemodynamic recordings obtained in NTG and AC8TG mice. Isoproterenol (ISO) was injected IP at the indicated concentrations during hemodynamic recording. **P*<0.05, ***P*<0.01; ****P*<0.001; ****P*<0.001 *vs* NTG at the same condition (Student unpaired *t*-tests).

Figure 5. Cardiac adenylyl cyclase overexpression accelerates deterioration of cardiac function with ageing. A, B, C, D. Echocardiographic assessment of global LV function in conscious 2- (n=13),

6- (n=12) and 12-mo-old (n=20) NTG and 2- (n=5), 6- (n=8) and 12-mo-old (n=20) AC8TG mice. The parameters measured in NTG (○) and AC8TM (●) mice were: (**A**) heart rate (HR) in beats/min; (**B**) LV end systolic diameter (LVESD) in mm; (**C**) LV ejection fraction (LVEF) in %. (**D**) LV anterior strain rates (StR, s^{-1}). The horizontal line indicates the mean value for each group. **P*<0.05, ***P*<0.01, ****P*<0.001 *vs* NTG (5-20 animals were analyzed in each group, as indicated on the figure; statistical significance was determined using one-way ANOVA followed by Newman-Keuls post-hoc test).

Figure 6. Deterioration of cardiac morphology by ageing is accelerated by AC8 overexpression. A. Macro histological analysis of heart cross-sections from 2-, 6- and 12-mo-old mice. Hematoxylin/eosin staining. Representative images from 5 animals for each group. **B, C.** Slot-plot showing the relative mRNA expression normalized to β-actin mRNA of β-MHC (**B**) and ANP (**C**) in NTG (○) and AC8TG (●) mice. 10 animals were analyzed in each group. **D.** Histological analysis of myocardial tissue from 2- and 12-mo-old NTG and AC8TG animals. Heart cross sections. Scale bars: 100 µm. **Upper panel:** hematoxylin/eosin. **Middle panel:** WGA-Alexa Fluor 488 staining showing cardiomyocytes size. **Lower panel:** Sirius red staining showing myocardial fibrosis (red). Representative images of 5 animals from each group. Bar: 100 µm. **E.** Quantification of histological analysis. **Left panel**: scarred plot of cardiomyocyte area. Two hundred individual measurements were performed on 5 sections for each animal. Five animals per group were analyzed; each point represents the mean value per animal. The horizontal line indicates the mean value for each group. ****P*<0.001 (one-way ANOVA followed by Newman-Keuls post-hoc test); #P<0.5; ##P<0.01(Student unpaired *t*-tests). **Middle and right panel:** relative quantification of fibrosis based on 5 sections of the endocardial and epicardial area for each animal. ***P*<0.01; ****P*<0.001 (one-way ANOVA followed by Newman-Keuls post-hoc test).

Figure 7. Schematic showing proposed changes of cAMP/PKA signaling in 2-mo-old and 12-mop-old NTG or AC8TG animals. A. In healthy cardiomyocytes major cAMP/PKA events are confined in the interspace T-tubule/junctional reticulum controlling inotropic response via LTCC and RyR phosphorylation. **B.** In AC8TG, cAMP produced by AC8 is confined at the level of longitudinal reticulum, having access to the SERCA2a/PLN compartment, but not to LTCC compartment. SERCA2A/PLN compartment is delimited by PDE1A&C, PDE3B and PDE4D. The benefit effect of PLN phosphorylation in AC8TG is hampered by phosphorylation GSK3α&β, apparently located in the same compartment. **C.** In early compensated age-related dysfunction, the effective junctional reticulum/T-tubule microdomain confining is lost, leading to channeling of cAMP towards longitudinal reticulum and increased PLN phosphorylation in order to compensate for the loss of contractile function and degradation of tissue condition. However, GSK3 phosphorylation hampers this compensating adaptation via induction of hypertrophy-, fibrosis- and ageing-related pathways.

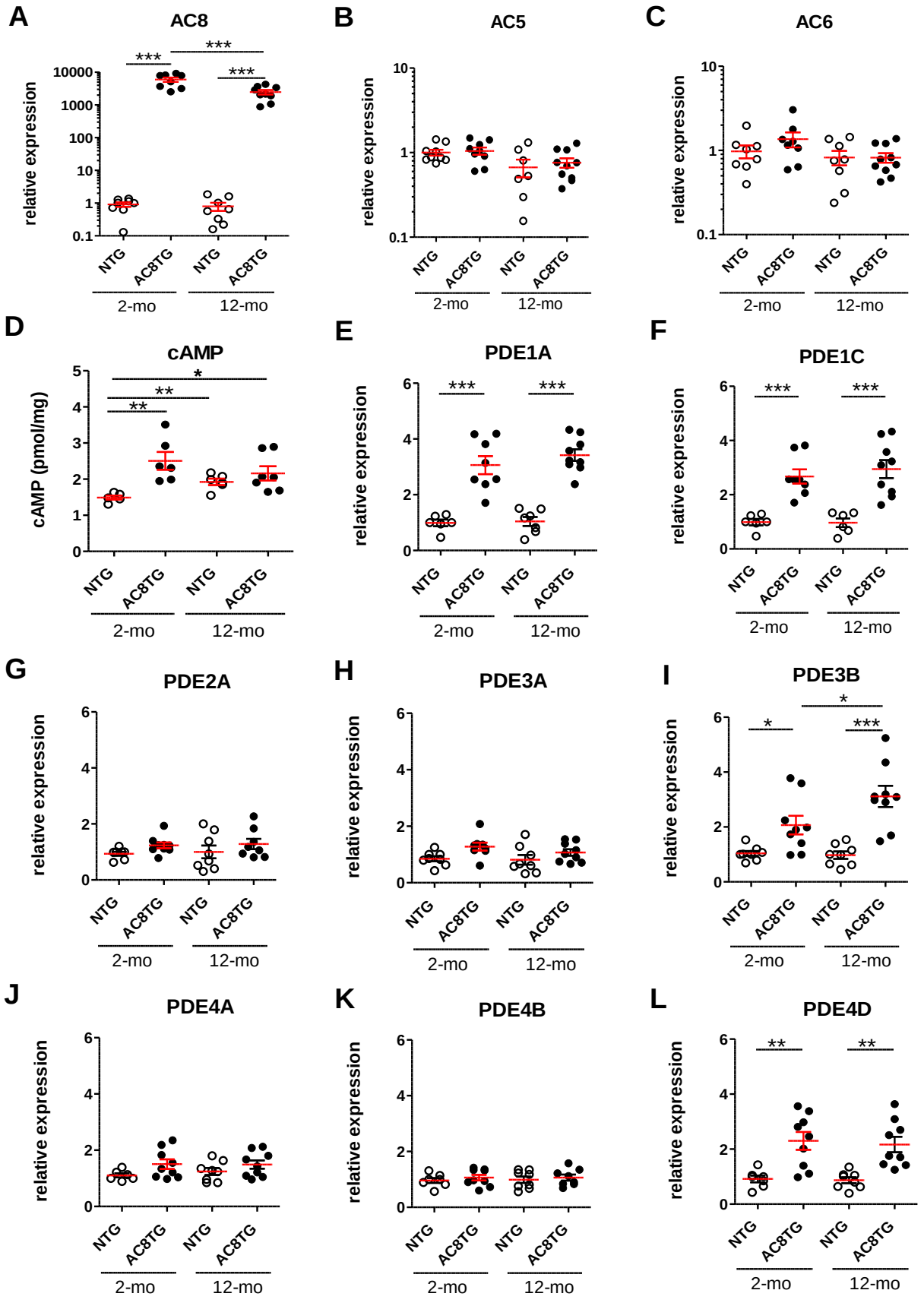
A
AC8
relative expression
10000
1000
100
10
1
0.1
***
***
***
NTG
AC8TG
NTG
AC8TG
2-mo
12-mo
B
AC5
relative expression
10
1
0.1
NTG
AC8TG
NTG
AC8TG
2-mo
12-mo
C
AC6
relative expression
10
1
0.1
NTG
AC8TG
NTG
AC8TG
2-mo
12-mo
D
cAMP
cAMP (pmol/mg)
5
4
3
2
1
0
*
**
**
NTG
AC8TG
NTG
AC8TG
2-mo
12-mo
E
PDE1A
relative expression
6
4
2
0
***
***
NTG
AC8TG
NTG
AC8TG
2-mo
12-mo
F
PDE1C
relative expression
6
4
2
0
***
***
NTG
AC8TG
NTG
AC8TG
2-mo
12-mo
G
PDE2A
relative expression
6
4
2
0
NTG
AC8TG
NTG
AC8TG
2-mo
12-mo
H
PDE3A
relative expression
6
4
2
0
NTG
AC8TG
NTG
AC8TG
2-mo
12-mo
I
PDE3B
relative expression
6
4
2
0
*
*
***
NTG
AC8TG
NTG
AC8TG
2-mo
12-mo
J
PDE4A
relative expression
6
4
2
0
NTG
AC8TG
NTG
AC8TG
2-mo
12-mo
K
PDE4B
relative expression
6
4
2
0
NTG
AC8TG
NTG
AC8TG
2-mo
12-mo
L
PDE4D
relative expression
6
4
2
0
**
**
NTG
AC8TG
NTG
AC8TG
2-mo
12-mo

Figure 1

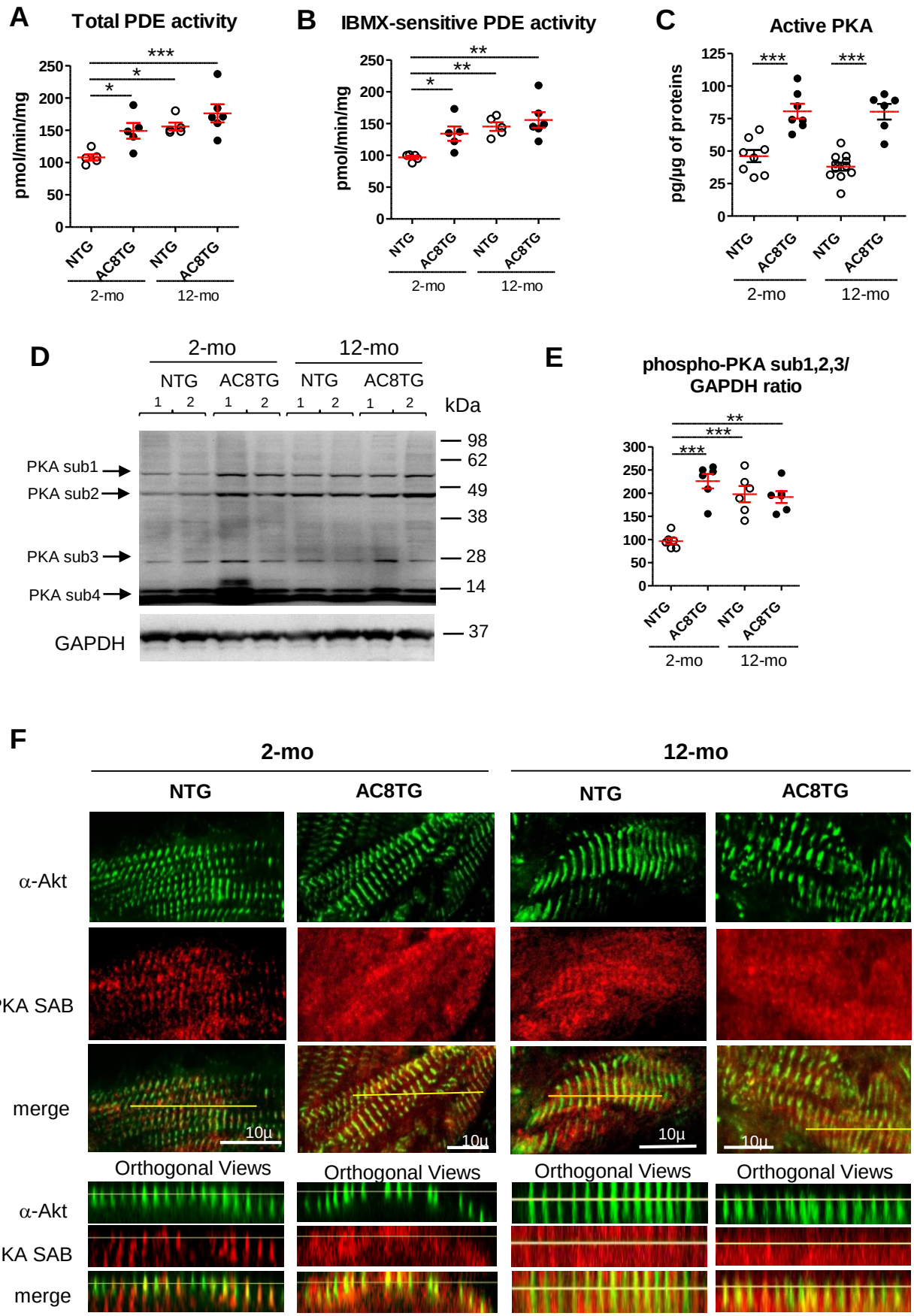
A
Total PDE activity
pmol/min/mg
250
200
150
100
50
0
***
*
*
NTG
AC8TG
NTG
AC8TG
2-mo
12-mo
B
IBMX-sensitive PDE activity
pmol/min/mg
250
200
150
100
50
0
**
**
*
NTG
AC8TG
NTG
AC8TG
2-mo
12-mo
C
Active PKA
pg/µg of proteins
125
100
75
50
25
0
***
***
NTG
AC8TG
NTG
AC8TG
2-mo
12-mo
D
2-mo
12-mo
NTG
AC8TG
NTG
AC8TG
1
2
1
2
1
2
1
2
kDa
PKA sub1
PKA sub2
PKA sub3
PKA sub4
GAPDH
98
62
49
38
28
14
37
E
phospho-PKA sub1,2,3/
GAPDH ratio
300
250
200
150
100
50
0
**
***
***
NTG
AC8TG
NTG
AC8TG
2-mo
12-mo
F
2-mo
12-mo
NTG
AC8TG
NTG
AC8TG
α-Akt
pPKA SAB
merge
10µ
10µ
10µ
10µ
Orthogonal Views
Orthogonal Views
Orthogonal Views
Orthogonal Views
α-Akt
pPKA SAB
merge

Figure 2

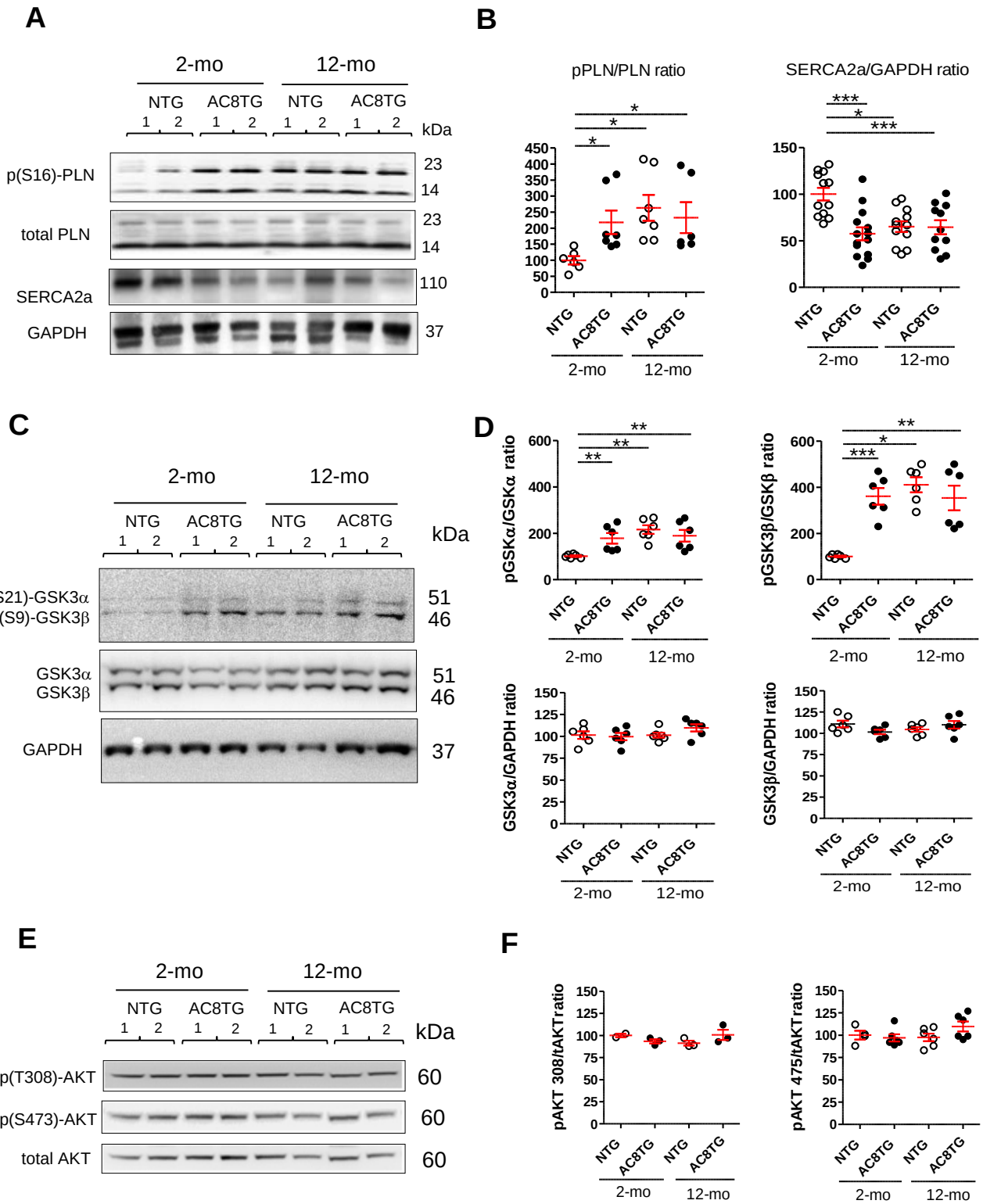
A
2-mo
12-mo
NTG
AC8TG
NTG
AC8TG
1 2 1 2 1 2 1 2
kDa
p(S16)-PLN
23
14
total PLN
23
14
SERCA2a
110
GAPDH
37
B
pPLN/PLN ratio
SERCA2a/GAPDH ratio
NTG
AC8TG
NTG
AC8TG
2-mo
12-mo
C
2-mo
12-mo
NTG
AC8TG
NTG
AC8TG
1 2 1 2 1 2 1 2
kDa
p(S21)-GSK3α
p(S9)-GSK3β
51
46
GSK3α
GSK3β
51
46
GAPDH
37
D
pGSKα/GSKα ratio
pGSK3β/GSKβ ratio
GSK3α/GAPDH ratio
GSK3β/GAPDH ratio
NTG
AC8TG
NTG
AC8TG
2-mo
12-mo
E
2-mo
12-mo
NTG
AC8TG
NTG
AC8TG
1 2 1 2 1 2 1 2
kDa
p(T308)-AKT
60
p(S473)-AKT
60
total AKT
60
F
pAKT 308/tAKT ratio
pAKT 475/tAKT ratio
NTG
AC8TG
NTG
AC8TG
2-mo
12-mo

Figure 3

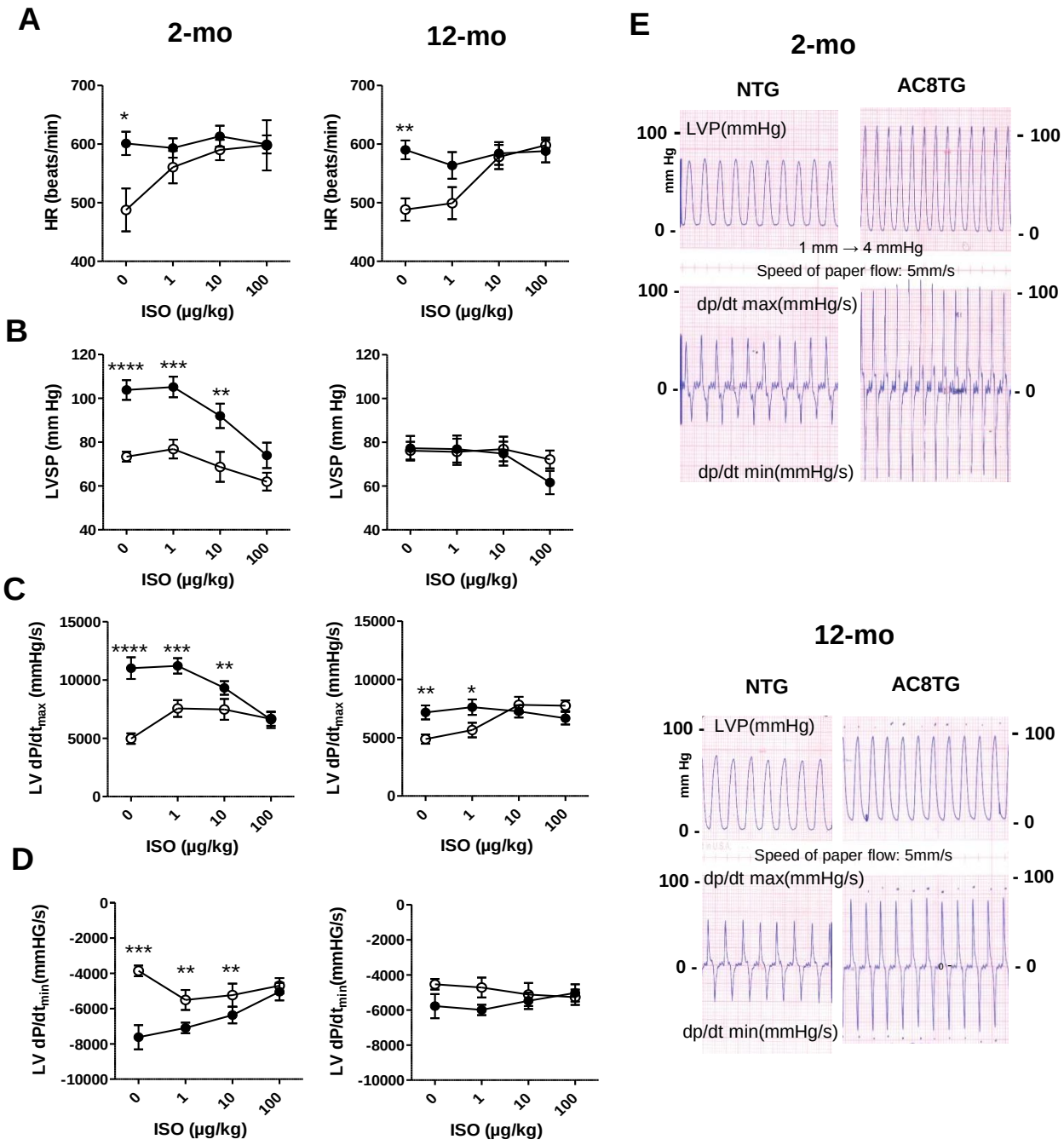
A
2-mo
12-mo
HR (beats/min)
ISO (μg/kg)
B
LVSP (mm Hg)
C
LV dP/dtmax (mmHg/s)
D
LV dP/dtmin(mmHG/s)
E
2-mo
NTG
AC8TG
LVP(mmHg)
mm Hg
1 mm → 4 mmHg
Speed of paper flow: 5mm/s
dp/dt max(mmHg/s)
dp/dt min(mmHg/s)
12-mo

Figure 4

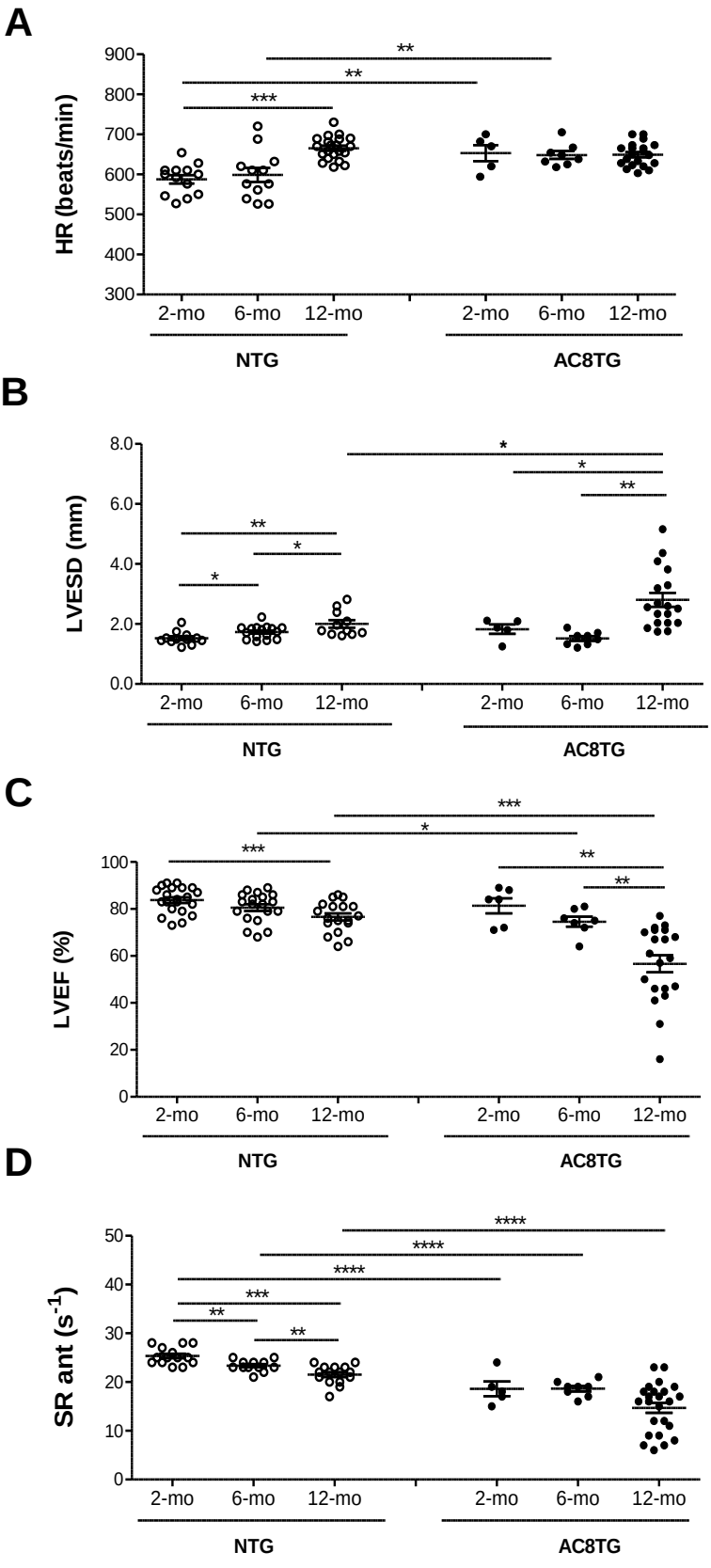
A
HR (beats/min)
900
800
700
600
500
400
300
**
**
***
2-mo
6-mo
12-mo
2-mo
6-mo
12-mo
NTG
AC8TG
B
LVESD (mm)
8.0
6.0
4.0
2.0
0.0
*
*
**
**
*
*
2-mo
6-mo
12-mo
2-mo
6-mo
12-mo
NTG
AC8TG
C
LVEF (%)
100
80
60
40
20
0
***
*
***
**
**
2-mo
6-mo
12-mo
2-mo
6-mo
12-mo
NTG
AC8TG
D
SR ant (s-1)
50
40
30
20
10
0
****
****
****
***
**
**
2-mo
6-mo
12-mo
2-mo
6-mo
12-mo
NTG
AC8TG

Figure 5

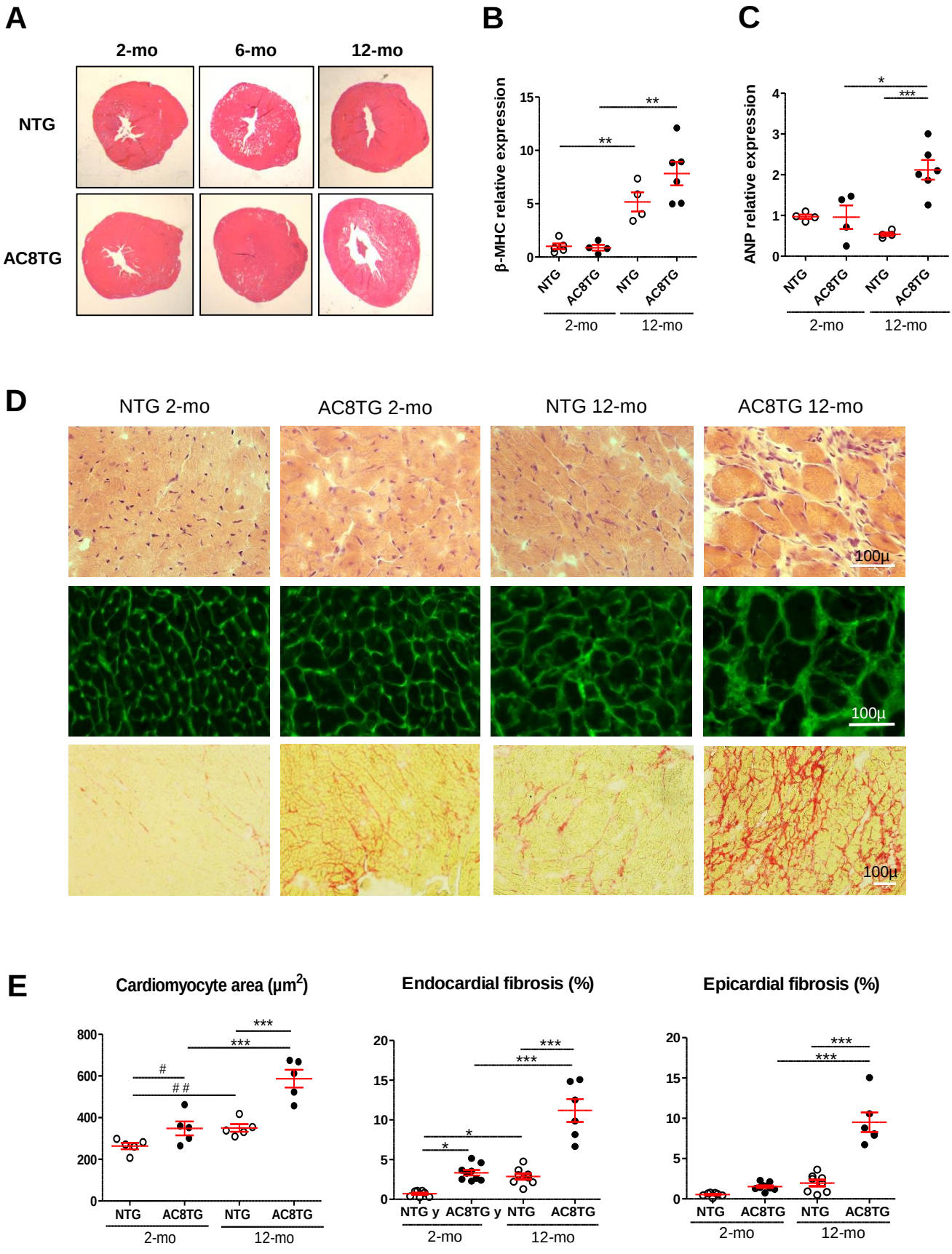
A
2-mo
6-mo
12-mo
NTG
AC8TG
B
β-MHC relative expression
15
10
5
0
**
**
NTG
AC8TG
NTG
AC8TG
2-mo
12-mo
C
ANP relative expression
4
3
2
1
0
*
***
NTG
AC8TG
NTG
AC8TG
2-mo
12-mo
D
NTG 2-mo
AC8TG 2-mo
NTG 12-mo
AC8TG 12-mo
100µ
100µ
100µ
E
Cardiomyocyte area (µm2)
800
600
400
200
0
***
***
#
##
NTG
AC8TG
NTG
AC8TG
2-mo
12-mo
Endocardial fibrosis (%)
20
15
10
5
0
***
***
*
*
NTG y
AC8TG y
NTG
AC8TG
2-mo
12-mo
Epicardial fibrosis (%)
20
15
10
5
0
***
***
NTG
AC8TG
NTG
AC8TG
2-mo
12-mo

Figure 6

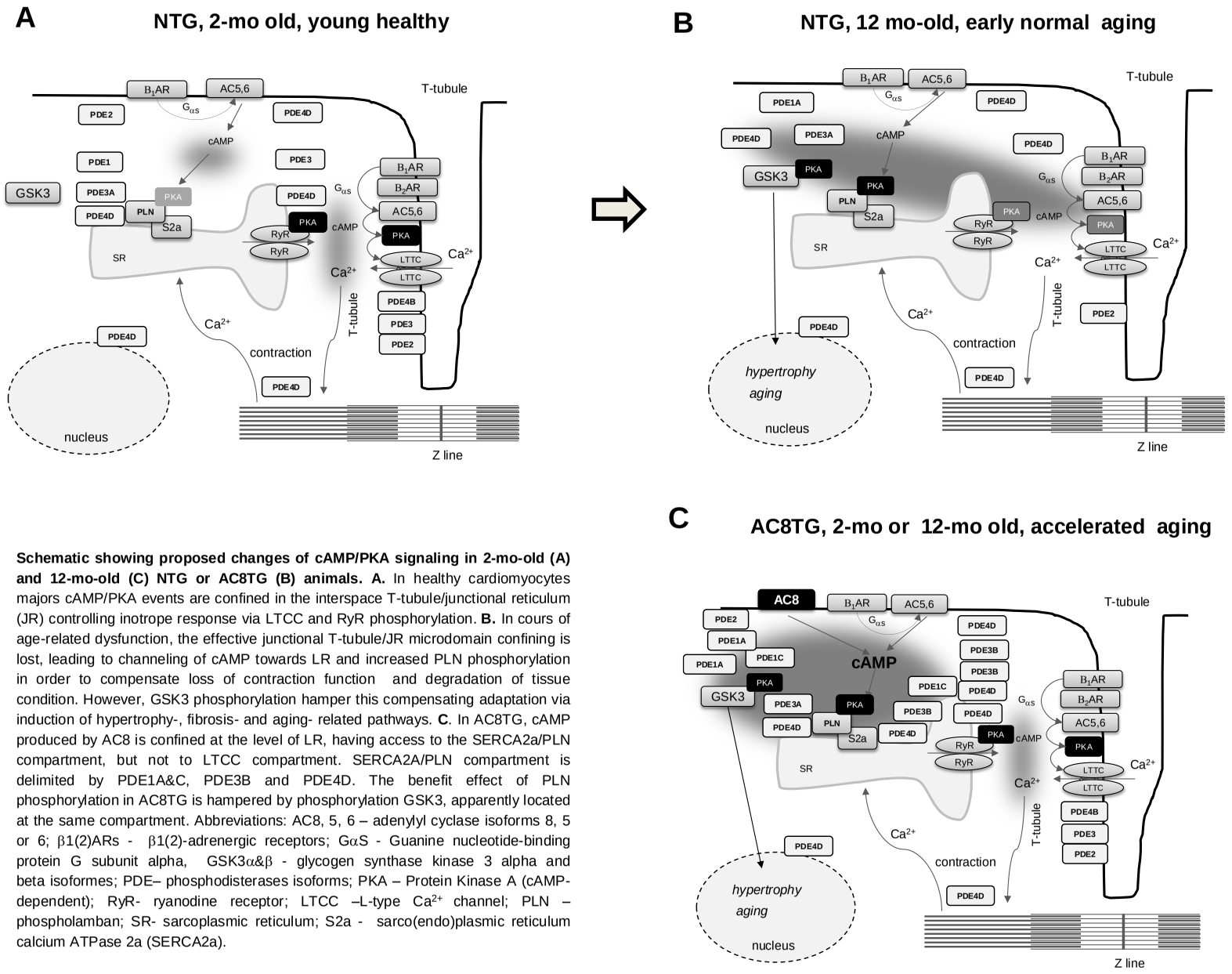

Schematic showing proposed changes of cAMP/PKA signaling in 2-mo-old (A) and 12-mo-old (C) NTG or AC8TG (B) animals. A. In healthy cardiomyocytes majors cAMP/PKA events are confined in the interspace T-tubule/junctional reticulum (JR) controlling inotrope response via LTCC and RyR phosphorylation. **B.** In cours of age-related dysfunction, the effective junctional T-tubule/JR microdomain confining is lost, leading to channeling of cAMP towards LR and increased PLN phosphorylation in order to compensate loss of contraction function and degradation of tissue condition. However, GSK3 phosphorylation hamper this compensating adaptation via induction of hypertrophy-, fibrosis- and aging- related pathways. **C**. In AC8TG, cAMP produced by AC8 is confined at the level of LR, having access to the SERCA2a/PLN compartment, but not to LTCC compartment. SERCA2A/PLN compartment is delimited by PDE1A&C, PDE3B and PDE4D. The benefit effect of PLN phosphorylation in AC8TG is hampered by phosphorylation GSK3, apparently located at the same compartment. Abbreviations: AC8, 5, 6 – adenylyl cyclase isoforms 8, 5 or 6; β1(2)ARs - β1(2)-adrenergic receptors; GαS - Guanine nucleotide-binding protein G subunit alpha, GSK3α&β - glycogen synthase kinase 3 alpha and beta isoformes; PDE– phosphodisterases isoforms; PKA – Protein Kinase A (cAMP-dependent); RyR- ryanodine receptor; LTCC –L-type Ca^{2+} channel; PLN – phospholamban; SR- sarcoplasmic reticulum; S2a - sarco(endo)plasmic reticulum calcium ATPase 2a (SERCA2a).

Figure 7

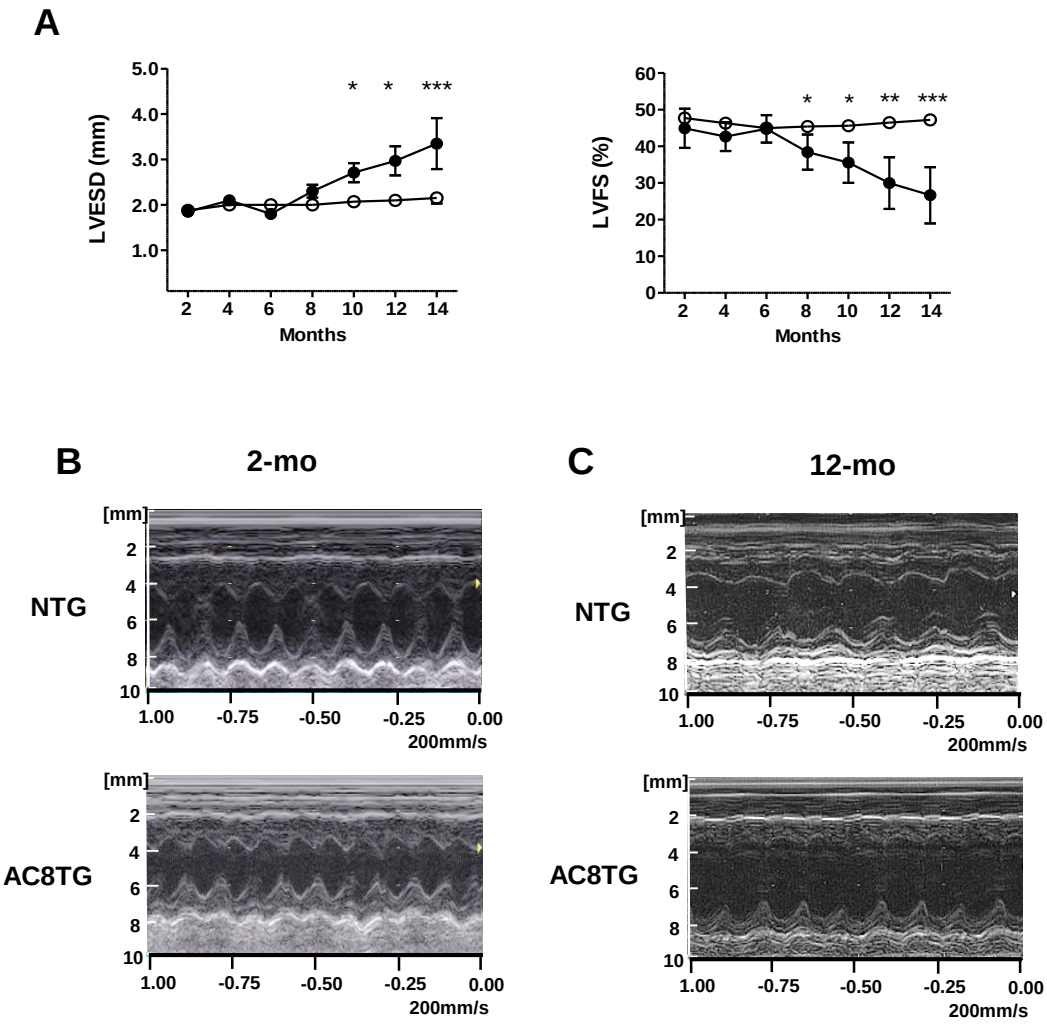
A
LVESD (mm)
5.0
4.0
3.0
2.0
1.0
* * ***
2 4 6 8 10 12 14
Months
LVFS (%)
60
50
40
30
20
10
0
* * ** ***
2 4 6 8 10 12 14
Months
B
2-mo
NTG
AC8TG
[mm]
2
4
6
8
10
1.00 -0.75 -0.50 -0.25 0.00
200mm/s
C
12-mo
NTG
AC8TG
[mm]
2
4
6
8
10
1.00 -0.75 -0.50 -0.25 0.00
200mm/s

Figure S1

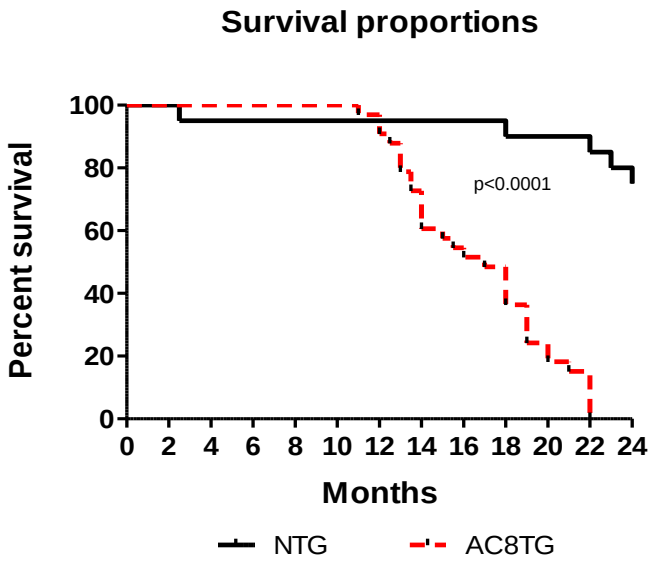
Survival proportions
Percent survival
100
80
60
40
20
0
0 2 4 6 8 10 12 14 16 18 20 22 24
Months
p<0.0001
NTG
AC8TG

Figure S2